BNL-99463-2013-TECH
C-A/AP/314;BNL-99463-2013-IR

Summary on the fundamental mode damper experiments of the 56 MHz SRF cavity

E. M. Choi

July 2008

Collider Accelerator Department
Brookhaven National Laboratory

U.S. Department of Energy
USDOE Office of Science (SC)

DISCLAIMER

BNL-81595-2008-IR

C-A/AP/#314
July 2008

Summary on the fundamental mode damper experiments of the 56 MHz SRF cavity

E. M. Choi and H. Hahn

Collider-Accelerator Department
Brookhaven National Laboratory
Upton, NY 11973

Summary on the fundamental mode damper experiments of the 56 MHz SRF cavity

E. M. Choi and H. Hahn

July 10, 2008

Abstract

This report summarizes the experimental results done with the fundamental damper for the 56 MHz prototype Cu cavity. Various measurements were done on the cavity including determination of the position of the fundamental damper and measurement of the frequency and Q factor changes while the damper is withdrawn. Prediction on the dissipated power while the damper is withdrawn was made by experiments.

1 Introduction

A 56 MHz superconducting quarter-wave cavity is being designed and fabricated as one path to increased luminosity in RHIC. The cavity will be installed in IP4, at 6.6 m from the crossing point and common to both beams. Injection and acceleration is done with the 28 MHz RF cavity system. In this phase, the 56 MHz cavity is heavily damped down to Q $\approx$ 300 by means of the "fundamental damper (FD)" to prevent beam instabilities. At store, the FD is removed and the cavity is beam excited with the nominal 2×0.3 A to 2.5 MV and is amplitude and phase controlled with a 1 kW RF source. Table 1 shows the cavity parameters of the Superconducting RF 56 MHz cavity.

The FD is constructed as a 8 by 8 cm loop in the cavity which is connected to a 50 Ω termination at room temperature. The beam delivers a power into the coupler which is a function of its degree of insertion and the degree of detuning of the cavity with respect to the beam. With full insertion and no detuning, this power is 12 kW. During its removal the power flow can increase by an order of magnitude. Minimizing the power flow into the termination and maintaing a low enough Q for damping as the cavity frequency is kept below the beam frequency at store is a primary design consideration.

Table 1: Summary of the 56 MHz SRF cavity parameters

Parameter	Values
Frequency	56.298 MHz
Voltage	2.5 MV
Superconducting surface resistance	10 nOhm
Power dissipated to LHe (4.2 K)	42 W
Q factor	1.8×10^9
Stored energy	221 J (From MWS)
R over Q (accelerator definition)	79.9 (From MWS)

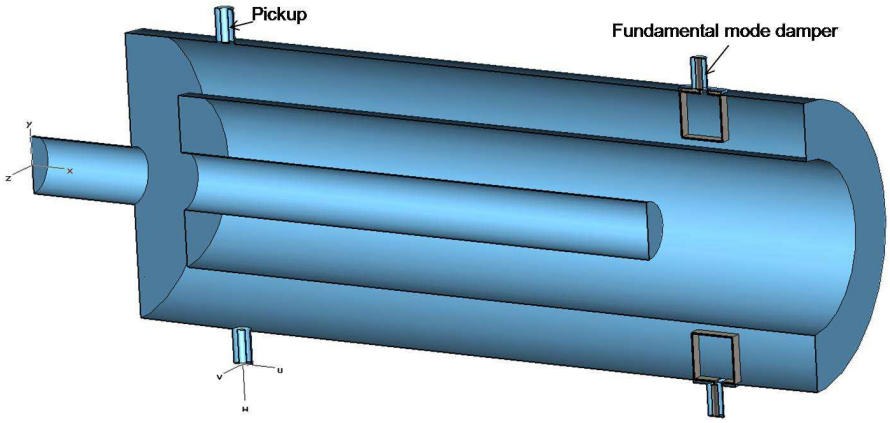

Figure 1: The model of the 56 MHz prototype Cu cavity. The fundamental mode damper is seen towards the end of the cavity.

2 The fundamental mode damper location

The fundamental mode damper (FD) for the 56 MHz SC RF cavity was chosen to be an inductive coupler so that for maximum coupling it will be situated close to the end of the cavity. The withdrawal of the loop results in a change of the resonance frequency which could lead to several problems including the frequency crossover to the beam frequency and maximum power dissipation to the damper load. It was found that the magnetic and electric fields at the damper location have an opposite effect on the frequency shift and the optimum is somewhere in between the maximum magnetic field region and the maximum electric field region. The frequency shift in the unwanted direction can be corrected by locating the fundamental damper properly so that the cavity frequency is maintained below the beam frequency to satisfy the Robinson stability criteria above transition at store.

The location of the FD was studied via MWS simulations and the measurements of the prototype Cu cavity. The simulation model including the FD is shown in Fig. 1. The use of two identical dampers in the MWS allows to simplify the simulation problem by introducing E and H symmetry planes in boundaries. The axial location of the FD with fully inserted loop was parametrically varied in the experiment and the simulation and the results of the frequency shift and the Q factors are shown in Fig. 2. The measurements are in a good agreement with the simulation results. The frequency shift is defined as the cavity frequency with the damper inserted minus the empty cavity frequency.

At the cavity end, the damper loop increases the frequency so that its withdrawal would lower the cavity frequency and exceed the tuning capability of the slow tuner since after the withdrawal, the slow tuner must bring the cavity within a couple of hundreds of Hertz of the beam harmonic frequency, depending on the required voltage and the beam current. Based on the axial location study on the fundamental mode damper, one can approximately locate the axial position of the FD. However, it is now necessary to study

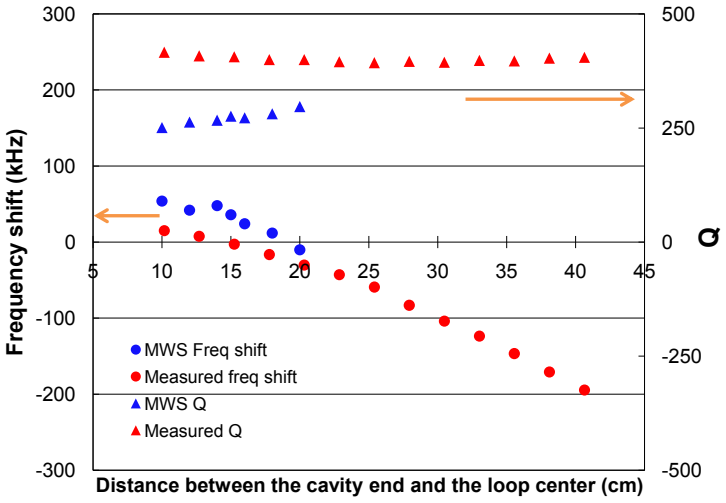

Figure 2: The measured and simulated frequency shift and Q factors as a function of the cavity axial position

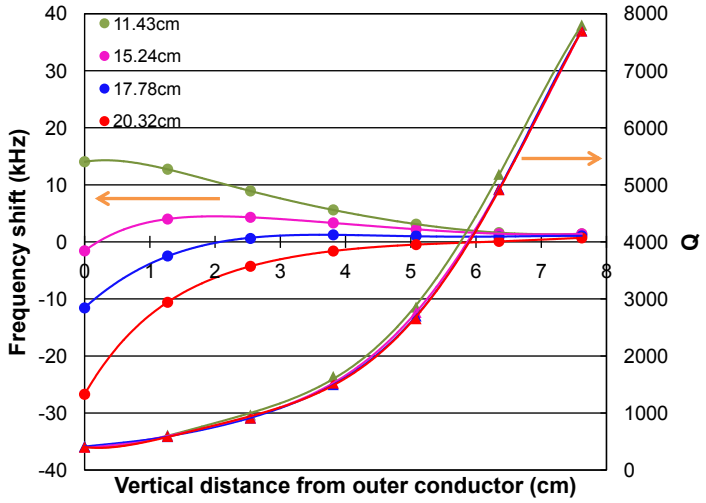

Figure 3: The measured frequency shift and the Q factors as a function of the damper vertical position (same as withdrawing the damper) at different axial locations.

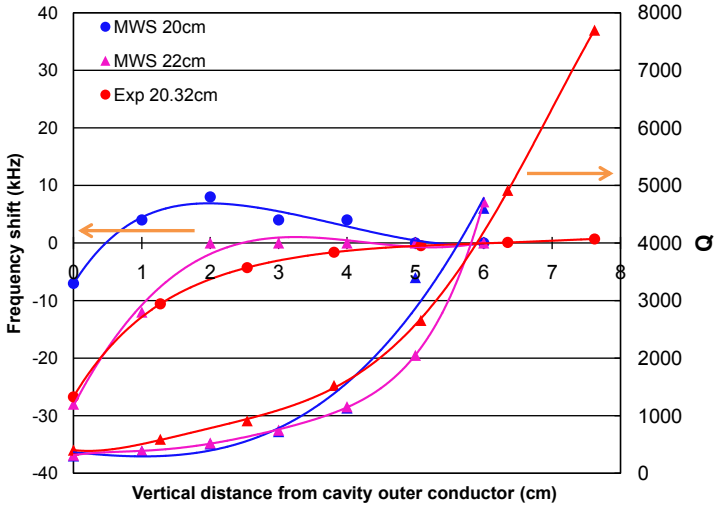

Figure 4: The measured frequency shift and Q factors at vertical position compared to the MWS simulations (same as withdrawing the damper)

the effect of the vertical damper position in more detail. The measured cavity frequency and the Q-value as a function of the vertical location of the damper are shown in Fig. 3 at various axial locations.

The measurements on the location of the FD are compared with the MWS simulations and plotted in Fig. 4. The measurements are well matched with the simulations. With the goal of preventing the cavity frequency passing the beam frequency, one can finalize the axial location of the fundamental mode damper at 20.32 cm (8 in.) where the frequency shift never goes above 0.

3 The dissipated power to the load

Minimizing the power extracted from the cavity and dissipated in the load is important since it comes from the beam and to maintain its energy and orbit must be compensated by the 28 MHz accelerating cavities of the storage ring. The power to the load can be estimated from the experimentally measured external Q factor for the damper. Interpretation of the results is based on the parallel circuit model for the cavity and the damper in Fig. 5. Absolute values for the circuit elements, cavity inductance L and capacitance C require the use of R/Q from either bead pull measurements or simulations. For our purpose, we used the R/Q from the MWS simulations. The bare cavity circuit values are

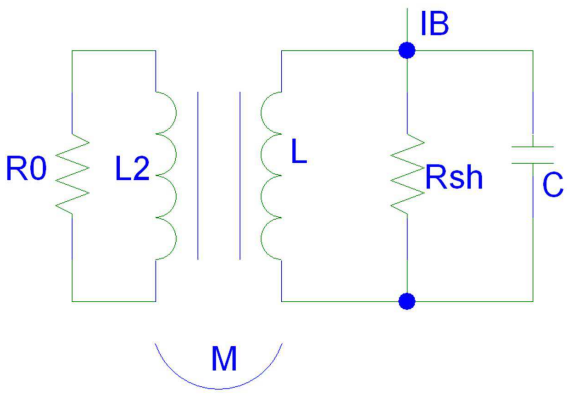

Figure 5: The circuit representation of the cavity with the damper.

found from the simulated

$$\frac{R_{acc}}{Q} = 2\sqrt{\frac{L}{C}}. \tag{1}$$

together with the measured $\omega_0 = 1/\sqrt{LC}$. One should note that R_{acc}/Q in the Eq. 1 is defined in the accelerator form, which is twice larger than circuit definition. (That's why 2 appears in Eq. 1 on the right hand side.)

The R/Q in Table 1, given in the "acceleration" definition, and the f_0 of 56.25 MHz can be plugged into the equations, and the resultant "circuit" L value is 113 nH. The other circuit elements, M and L_2, were measured and are discussed in the next section. The intrinsic quality factor of the cavity defines $Q_0 = R_{sh}/\omega_0 L$, where ω_0 is the cavity resonant frequency. The external Q factor, $Q_{ext}^{-1} = Q_0^{-1} - Q_{load}^{-1}$, defines the damping load $R_x = \omega_0 L Q_{ext}$, which is distinct from the physical load R_0.

The circuit shunt impedance when the damper is present is expressed as

$$Z_c^{-1} = \left[j\omega L + \frac{(\omega L)^2}{(R_0 + j\omega L_2)} \right]^{-1} + R_{sh}^{-1} + j\omega C \tag{2}$$

and the damping load is

$$R_x^{-1} = Re\left[j\omega L + \frac{(\omega L)^2}{(R_0 + j\omega L_2)} \right]^{-1}. \tag{3}$$

The beam induced voltage in the cavity is as follows [1]

$$V_c = \frac{Z_c(2I_B)}{\sqrt{2}} \tag{4}$$

where the voltage and impedance are expressed in the circuit definition and I_B is the time averaged beam current. The power dissipated into the load termination is given by

$$P = \frac{V_c^* \cdot V_c}{R_x} = 2\frac{(ReZ_c)^2 I_B^2}{R_x}. \tag{5}$$

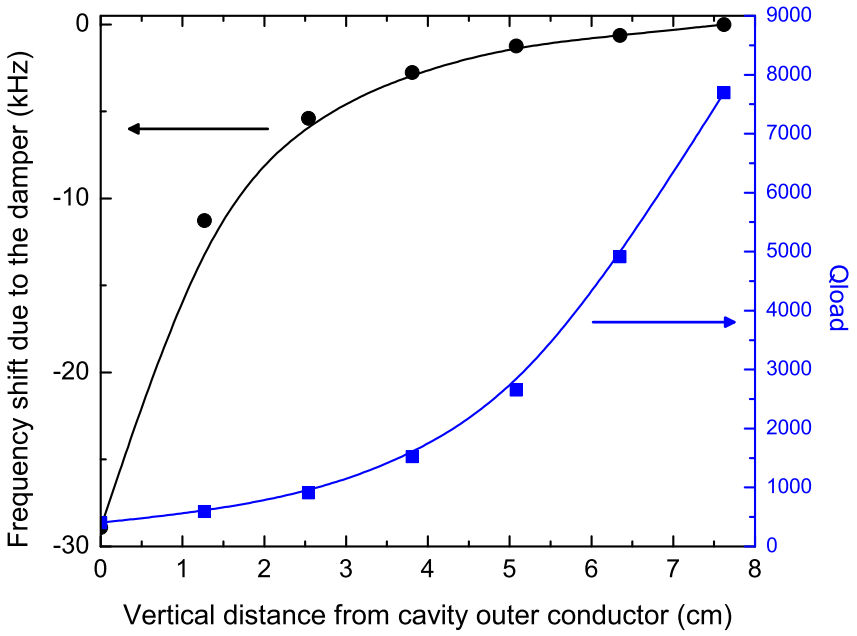

Figure 6: The frequency shift and the loaded Q.

The cavity will be located in the common area IP4, which results in doubling the beam current to 0.6 A for this case. All circuit values have been measured so that, in principle, the power dissipated into the load can be calculated from the above equations. A simpler and probably more reliable method involves the measurement of the loaded Q_{load} with the damper inserted.

3.1 The Q and f of the cavity with damper

The loaded cavity impedance can be summarily be represented by the expression

$$Z_c = \frac{\omega_0 L}{Q_{load}^{-1} - j\Delta} \tag{6}$$

with $\Delta = \left(\frac{\omega}{\omega_0} - \frac{\omega_0}{\omega}\right) \approx \frac{2(\omega-\omega_0)}{\omega_0}$. Here, ω represents the beam frequency and is kept constant at store, but the cavity resonance ω_0 is allowed to change when the damper is withdrawn. The Δ represents the normalized frequency offset between beam and actual cavity resonance. The power dissipated into the load can now be written in terms of the R/Q from simulation and the measured Q factors from Eq. 3, Eq. 4, Eq. 5 as

$$P = \frac{2R_{sh}}{Q_0} \frac{Q_{load}^2}{Q_{ext}\left[1 + (Q_{load}\Delta)^2\right]^2} I_B^2 \tag{7}$$

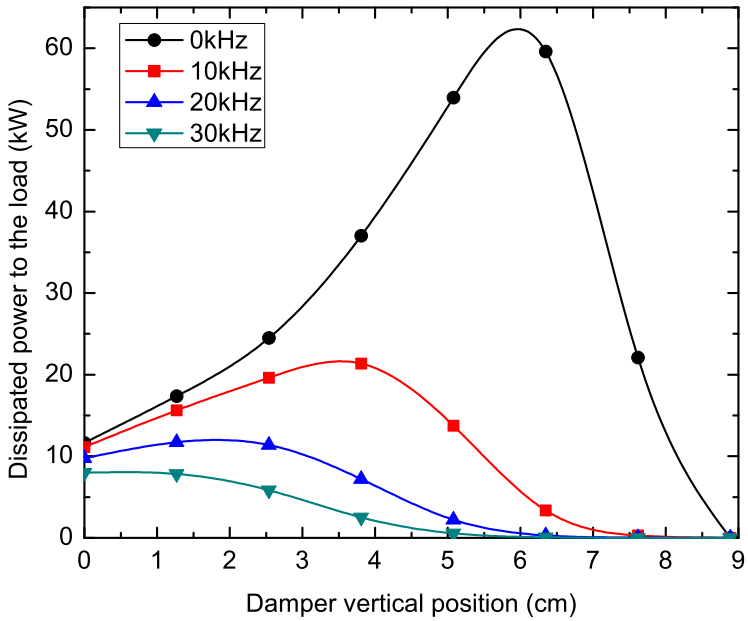

Figure 7: The dissipated power to the 50 Ω load as a function of the vertical damper position without considering the frequency shift due to the damper. Each curve represents the detuning value specified in the legend.

3.2 The power dissipated to the load

Fig. 6 shows experimental results of the frequency shift and loaded Q values with 50 Ω termination as a function of the damper vertical position which is the case of the damper withdrawn. The frequency shift is measured as the difference in frequency between the empty cavity resonant frequency and the damper loaded cavity resonant frequency. The axial position of the damper center is located 20 cm away from the end of the cavity. As shown in the plot, the frequency shift goes from -30 kHz to 0 kHz when the damper is withdrawn. The negative frequency shift is needed since the cavity frequency should be lower than the beam frequency after transition. A Q of 402 was measured with the damper fully inserted, and Q increases as the damper is withdrawn to an unloaded Q. From the measurements of the frequency shift and the Q values, one can plot the dissipated power to the load. Fig. 7 plots the dissipated power to the 50 Ω load assuming the constant cavity frequency with some detuning values Δ. As shown in Fig. 7, the maximum power during withdrawng at 0 detuning is around 60 kW. Since the dissipated power to the load comes from the beam energy, the power taken from the beam must be compensated by other cavities. In order to minimize the power to be compensated, some detuning may be necessary. With 10 kHz detuning, the maximum power can be decreased to 20 kW. As

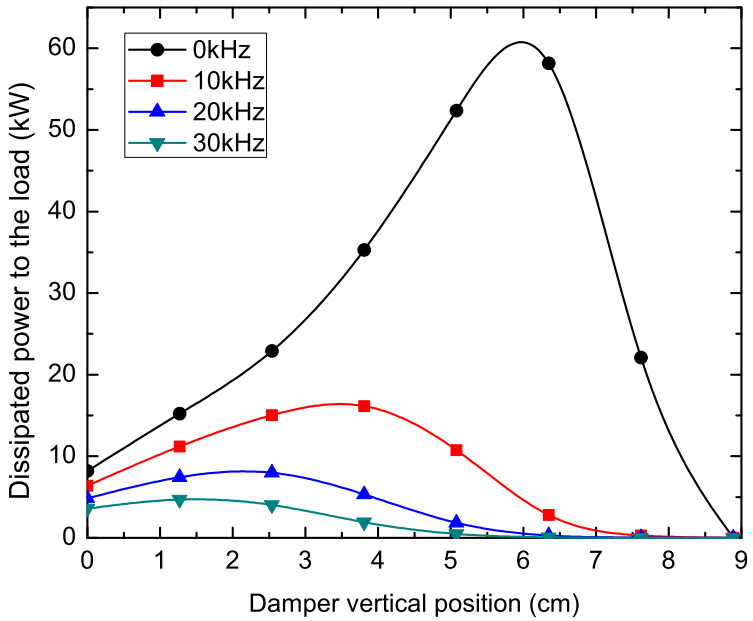

Figure 8: The dissipated power to the 50 Ohm load as a function of the vertical damper position with considering the frequency shift due to the damper. Each curve represents the detuning value specified in the legend.

the cavity is detuned more, the maximum power favorably decreases, but the slow tuner capability sets a limit.

Fig. 8 shows the dissipated power to the 50 Ω load when considering the frequency shift due to the presence of the damper with some detuning values added. Since the damper presence changes the cavity frequency at different damper vertical positions, an extra frequency detuning value at each location will be introduced. Large detuning occurs when the damper is fully inserted and the extra frequency shift results in a lowering of the dissipated. Providing a 10 kHz detuning leads here to a maximum dissipated power of around 16 kW during withdrawl. One should notice that the power when the damper is fully inserted is 11 kW without the frequency shift and 6.4 kW with the frequency shift included. Therefore, the power that should be compensated from other cavities can be reduced.

4 Cavity circuit parameters

Making performance estimates for the FD depends primarily on the measurements with the full-size Cu prototype but equally on their interpretation by means of an equivalent

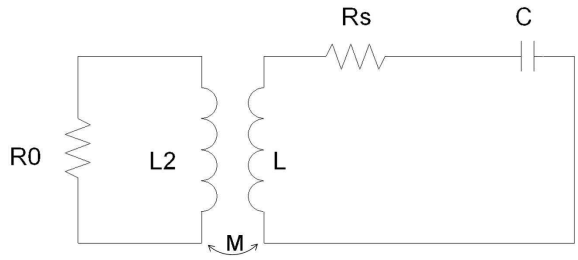

Figure 9: The fundamental damper equivalent circuit.

circuit. Depending on the task, the standard parallel circuit or the mathematically simpler series circuit shown in Fig. 9 is appropriate.

Absolute values for the circuit elements, cavity inductance L and capacitance C require results for R/Q from Superfish or MWS simulations, but note that the simulations give results in the "acceleration" definition. The bare cavity circuit values for the inductance has been derived from the simulation in Table 1 and f_0=56.25 MHz to be L=113 nH. The resistor value is found as $R_s = \omega_0 L/Q_0$ from the intrinsic Q value of the bare cavity without inserted damper. The mutual inductance of the fundamental damper and the self inductance of the loop require further network analyzer measurements of the cavity assembled with the coupler.

4.1 Q measurement method

By having Q measured, the self inductance of the FD loop and the mutual inductance can be determined. The external Q of the circuit is

$$Q_{ext} = \frac{\omega_0 L}{R_x} \tag{8}$$

where R_x is the real part of the external impedance, Z_m, which can be found from following

$$Z_m = \frac{(\omega M)^2}{R_0 + j\omega L_2} \tag{9}$$

where M, L_2, and R_0 refer the mutual inductance, the loop self inductance, and the termination of the loop respectively. Therefore, Q_{ext} can be expressed as follows

$$Q_{ext} = \frac{\omega_0 L}{R_x} = \frac{\omega_0 L\left[(R_0)^2 + (\omega L_2)^2\right]}{(\omega_0 M)^2 R_0}. \tag{10}$$

We have measured loaded Q values at two different damper coaxial cable lengths with each case of two different R_0 cases, 50 Ω and 25 Ω. The damper coaxial cable length is between the loop and the load. The coaxial cable is attached right away at the end of the damper. The coaxial cable has a 50 Ω characteristic impedance.

Table 2 summarizes the external Q measurements at different cable lengths with different terminations. The impedance mismatch has to come in the equation for the 25 Ω termination cases of the different damper lengths.

For the long cable with the 25 Ω termination, the input impedance in the transmission line, R_0 in Eq. 9 has now real and imaginary parts due to the impedance mismatch. The input impedance, R_0 can now be represented as follows.

$$R_0 = R_T \frac{\left(R_{term} + jR_T \tan(\frac{2\pi l}{\lambda})\right)}{\left(R_T + jR_{term} \tan(\frac{2\pi l}{\lambda})\right)} \tag{11}$$

where R_T and R_{term} represent the characteristic impedance of the transmission line and the load impedance at a given position l from the load. λ is the frequency of the mode. For the 25 Ω load termination of the long cable, Eq. 11 becomes $R_0 = 28.21 + 15.18j$. Therefore, Eq. 9 can be expressed as

$$Z_m^{25\Omega} = \frac{(\omega M)^2}{28.21 + (\omega L_2 + 15.18)j} \tag{12}$$

The resulting Q_{ext} for the 25 Ω load in the long cable is

$$Q_{ext}^{long}(25\Omega) = \frac{\omega L}{Re(Z_m^{25\Omega})} = \frac{\omega L\left[28.21^2 + (\omega L_2 + 15.18)^2\right]}{(\omega M)^2 \times 28.21}. \tag{13}$$

And the Q_{ext} for the 50 Ω in the long cable, which is impedance matched case, is following.

$$Q_{ext}^{long}(50\Omega) = \frac{\omega L}{Re(Z_m^{50\Omega})} = \frac{\omega L\left[50^2 + (\omega L_2)^2\right]}{(\omega M)^2 \times 50}. \tag{14}$$

Therefore, the ratio of the Q_{ext}s between the 50 Ω and the 25 Ω, measured to be 402 and 663 respectively, gives the self inductance, L_2, of the damper loop expressed as follows

$$\frac{Q_{ext}^{long}(50\Omega)}{Q_{ext}^{long}(25\Omega)} = \frac{402}{663} = \frac{28.21}{50}\frac{50^2 + (\omega L_2)^2}{28.21^2 + (\omega L_2 + 15.18)^2}. \tag{15}$$

The result for the self inductance of the loop, L_2, is

$$\omega L_2 = 39.3\ \Omega; \quad L_2 = 112\ \texttt{nH}. \tag{16}$$

The self inductance of the loop is expected to remain the same as the long cable case. The same procedure is applied in the short damper coaxial length case. From Eq. 11,

Table 2: Q_{ext} measurements at two different damper coaxial cable lengths

	short cable (1 cm)	long cable (35 cm)
50 Ω	301	402
25 Ω	355	663

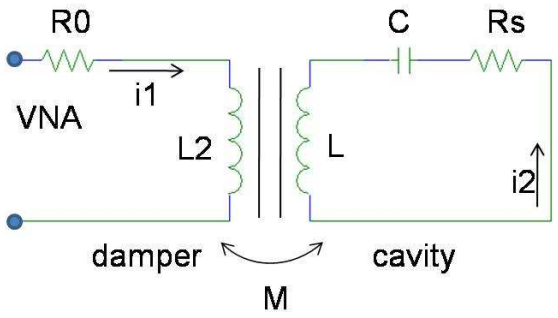

Figure 10: The circuit representation of the cavity with the damper seen by Vector Network Analyzer (VNA).

$R_0 = 25 + 0.45j$ is plugged in the Eq. 9. One can directly construct the following equation to get the L_2 alone and M.

$$\frac{Q_{ext}^{short}(50\Omega)}{Q_{ext}^{short}(25\Omega)} = \frac{301}{355} = \frac{1}{2}\frac{50^2 + (\omega_0 L_2)^2}{25^2 + (\omega_0 L_2 + 0.45)^2} \tag{17}$$

From Eq. 17, the self inductance of the damper loop for the short cable, L_2, is

$$\omega L_2 = 44.4\ \Omega; \quad L_2 = 126\ \texttt{nH}. \tag{18}$$

The consistent self inductance value of the damper loop is obtained from the long coaxial cable and the short coaxial cable. The mutual inductance, M, can be obtained from one of the external Q measurements (either Q_{50} or Q_{25}) with the resulting value for M = 8 nH.

4.2 S11 measurement

The S_{11} measurement can be used to determine the circuit parameters by directly converting the S_{11} to the impedance,

$$Z = R_0 \frac{1 - S_{11}}{1 + S_{11}} \tag{19}$$

where R_0 is 50 Ω.

The impedance seen by the Vector Network Analyzer (VNA) in the circuit representation shown in Fig. 10 is expressed as follows

$$Z = j\omega L + \frac{(\omega M)^2}{R_s + j\omega_0 L\Delta} \tag{20}$$

with $\Delta = \left(\frac{\omega}{\omega_0} - \frac{\omega_0}{\omega}\right)$. And the real part and imaginary part of the impedance are obtained from Eq. 20 and expressed as follows.

$$Re(Z) = \frac{(\omega M)^2 R_s}{R_s^2 + (\omega_0 L\Delta)^2} \tag{21}$$

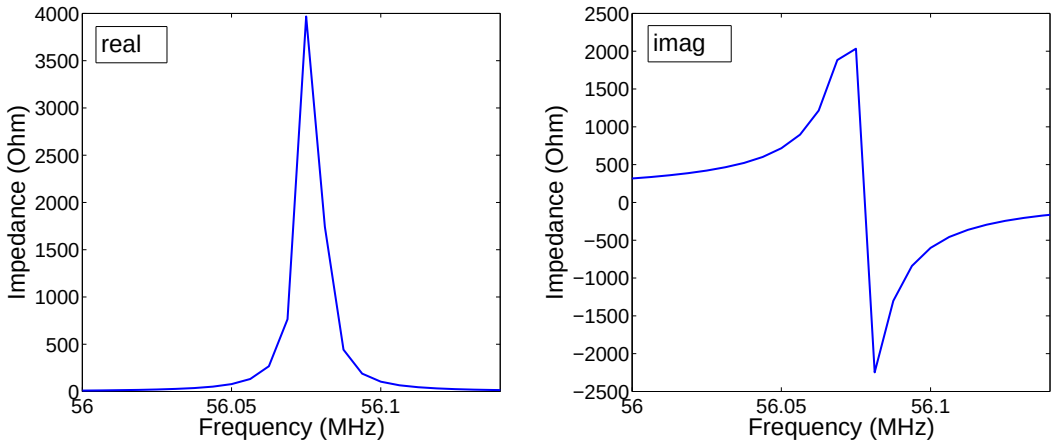

Figure 11: The measured impedance of real and imaginary parts from VNA of the long damper line

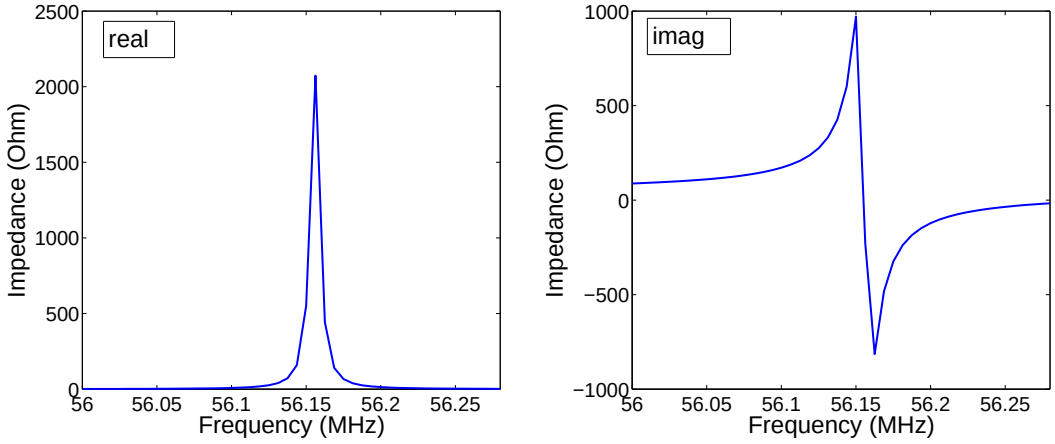

Figure 12: The measured impedance of real and imaginary parts from VNA of the short damper line.

$$Im(Z) = \omega L_2 - \frac{(\omega M)^2 (\omega_0 L \Delta)}{R_s^2 + (\omega_0 L \Delta)^2} \tag{22}$$

At resonance, $Re(Z)$ will give the mutual inductance M, and $Im(Z)$ will give the self inductance L_2, separately. For the S_{11} measurement, the different damper coaxial line lengths have been also used for the Q measurement method. Fig. 11 is the measured impedance from the VNA for the long damper line case (35 cm). One can obtain the mutual inductance and the self inductance of the damper loop at resonance from measurement using Eq. 21 and Eq. 22. The results for the M and the L_2 are 11 nH and 261 nH, respectively. Although not considered for the Nb cavity, the short damper line of 1 cm was also measured and plotted in Fig. 12. The mutual inductance and the self inductance of the 1 cm damper line are 4 nH and 92 nH, respectively.

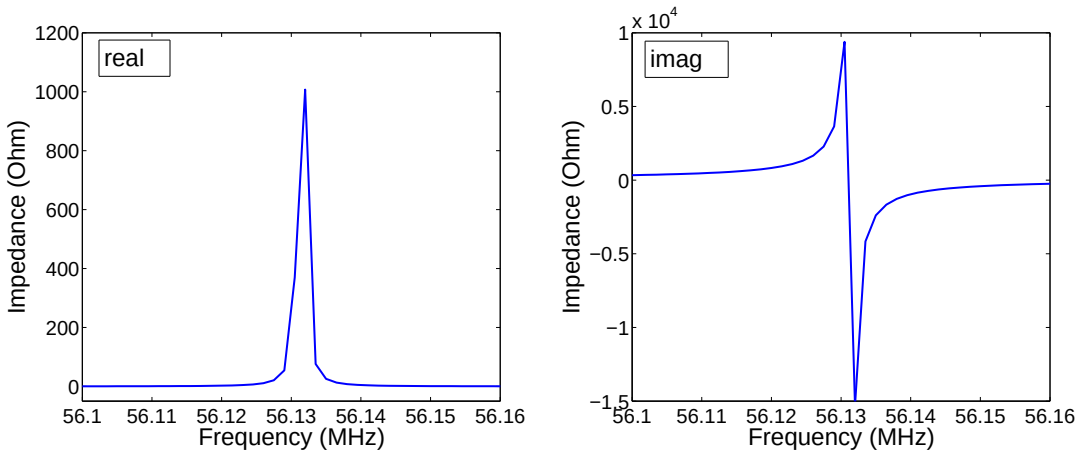

Figure 13: The simulated impedance of real and imaginary parts from MWS of the norminal damper line length of 35 cm.

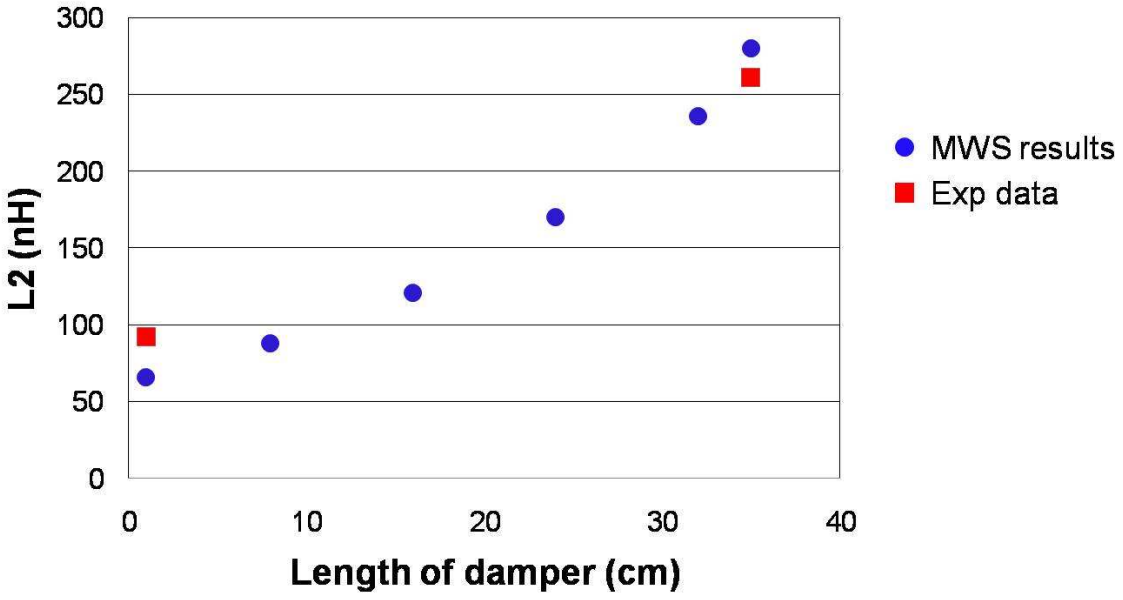

Figure 14: The comparison between the measurements and the simulations.

4.3 Simulation

The MWS simulation was done with different damper lengths and compared to the measurements. Fig. 13 is the S_{11} result from the MWS simulation for the 35 cm long damper line. The self inductance L_2 is 280 nH which is in a good agreement with the measurement. For the long damper line, the coaxial cable inductance which is around 150 nH is a part of the self inductance and added to the loop self inductance. (Note that from the short damper line, the L_2 is 92 nH. The additional coaxial cable inductance of 150 nH gives bigger inductance of the damper loop, which was observed in the long damper line measurements.) Fig. 14 plots the simulation results compared to the measurements. One can notice that the simulation matches very well to the measurement.

5 Conclusion

The fundamental damper is necessary for damping the fundamental mode during acceleration. The damper will be withdrawn at store to turn on the 56 MHz SRF cavity. The proper location of the fundamental damper was determined by the experiments. The dissipated power to the damper load was calculated based on measured external Q values. With the detuning of 20 kHz, the dissipated power can be kept below 20 kW. The cavity circuit parameters are studied via S_{21} and S_{11} measurements and compared to the MWS sumulations.

6 Acknowledgement

The authors would like to thank Dr. Ilan Ben-Zvi for his advice and helpful discussion.

References

[1] Padamsee, Knoblauch, and Hays, “RF superconductivity for Accelerators”, p 338.